Supplementary Material for "Learnable Skeleton-Based Medical Landmark Estimation with Graph Sparsity-Based Fiedler Regularizations"

Yao Wang[1], Jiahao Chen[1], Wenjian Huang[2], Pei Dong[3], and Zhen Qian[1,*]

[1] United-Imaging Research Institute of Intelligent Imaging, Beijing, China,
{yao.wang; zhen.qian}@cri-united-imaging.com
[2] Southern University of Science and Technology, Shenzhen, China,
[3] United-Imaging Intelligent, Beijing, China

1 Implementation Details

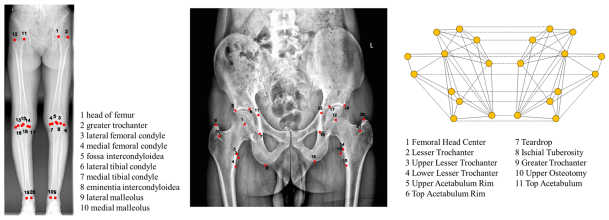

Fig. 1: Left: An example of the annotation of 20 lower limb landmarks utilized in this study. The lower dataset comprises 3342 images, with 2762 designated for training and 580 for testing. All images were resized to a resolution of 768×256 pixels. Right: An example of the annotation of 22 lower limb landmarks utilized in the pelvic dataset. In total, there are 2782 images, with 2224 images used for training and 558 for testing. The images are resized to a resolution of 1536×1536 pixels.

Table 1: Comparison of MRE Rates on pelvic dataset

Model	$L-Fhc$ $R-Fhc$	$L-Lt$ $R-Lt$	$L-Ult$ $R-Ult$	$L-Llt$ $R-Llt$	$L-Uar$ $R-Uar$	$L-Tar$ $R-Tar$	$L-Td$ $R-Td$	$L-It$ $R-It$	$L-Gt$ $R-Gt$	$L-Uo$ $R-Uo$	$L-Ta$ $R-Ta$	MRE
VDNet	43.400	15.413	20.862	12.638	12.333	30.688	5.969	40.991	13.303	16.404	**11.353**	
	36.785	32.714	24.596	37.059	18.323	23.236	5.960	22.236	18.926	27.071	23.229	22.431
VDNet	**7.781**	15.275	7.098	15.884	6.432	13.779	8.560	14.651	**7.727**	16.869	10.967	
+mask	9.356	12.804	11.017	12.413	8.120	12.700	8.899	**12.472**	12.639	17.415	12.417	11.603
GCN-58	9.750	8.879	9.174	9.837	7.866	10.635	14.417	14.395	14.126	12.939	12.900	
	10.701	13.200	8.741	11.941	8.281	12.195	10.990	19.302	8.894	**14.438**	14.648	11.738
GCN-69	8.870	**7.823**	7.568	10.269	7.423	11.862	12.255	**12.276**	14.111	16.016	**11.102**	
	7.702	10.680	9.472	12.876	**7.030**	12.154	8.860	14.831	11.432	21.040	14.084	11.352
GCN-full	9.389	11.585	**7.096**	13.936	7.709	10.918	9.122	16.031	11.670	18.171	11.745	
	14.360	**10.305**	7.292	**8.145**	14.736	17.243	12.208	16.651	13.873	14.990	17.877	12.502
Ours	8.279	8.608	7.133	**8.608**	**8.076**	**10.383**	**8.502**	13.741	9.670	**12.999**	12.754	
	8.767	10.589	**6.340**	**9.500**	9.410	**11.547**	**8.292**	14.606	**8.134**	14.787	**11.767**	**10.113**

Table 2: Comparison of MRE and SDR on ISBI 2015 challenge cephalograms dataset

Model	ISBI 2015 Challenge Test 1 Dataset					ISBI 2015 Challenge Test 2 Dataset				
	MRE	SDR				MRE	SDR			
		20	25	30	40		20	25	30	40
Chen[1]	11.7	86.67	92.67	95.54	98.53	14.8	75.05	82.84	88.53	95.05
Lin[2]	12.3	85.01	91.57	94.52	97.68	16.5	72.00	81.63	87.84	94.05
Zi[3]	11.6	86.25	92.18	**95.72**	**98.59**	**14.8**	74.26	82.11	**88.57**	**95.21**
Ours	**10.0**	**90.42**	**92.95**	94.49	96.35	15.0	**78.46**	**84.25**	87.86	92.32

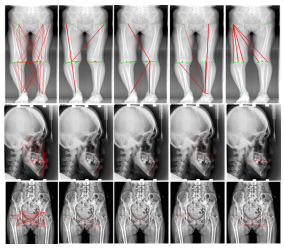

Fig. 2: Display of landmark detection results: Presented in pairs, each set showcases side-by-side outcomes. The left image represents the detection result obtained from a leading method (SOTA), while the right image illustrates the result generated by our method. The green dot denotes the ground truth landmark location, and the red dot signifies the predicted landmark location.

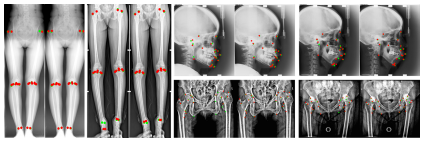

Fig. 3: Graph Structure Visualization: Green dots symbolize landmarks, while red lines represent edges, with the intensity of red denoting greater edge weights. The leftmost column illustrates the constructed graphs, highlighting the top three weighted edges for each landmark. The subsequent five columns to the right emphasize five specific landmarks, showcasing their most closely related neighbors through the five highest weighted edges.

References

1. Chen, R., Ma, Y., Chen, N., Lee, D., Wang, W.: Cephalometric landmark detection by attentive feature pyramid fusion and regression-voting. In: Medical Image Computing and Computer Assisted Intervention–MICCAI 2019: 22nd International Conference, Shenzhen, China, October 13–17, 2019, Proceedings, Part III 22. pp. 873–881. Springer (2019)
2. Lin, C., Zhu, B., Wang, Q., Liao, R., Qian, C., Lu, J., Zhou, J.: Structure-coherent deep feature learning for robust face alignment. IEEE Transactions on Image Processing **30**, 5313–5326 (2021). https://doi.org/10.1109/TIP.2021.3082319
3. Ye, Z., Yu, H., Li, B.: Uncertainty-aware u-net for medical landmark detection (2023)